ChemCatChem

The European Society Journal for Catalysis

Chemistry Europe

European Chemical Societies Publishing

Supported by GECATS GERMAN CATALYSIS SOCIETY

Accepted Article

Title: Regioselective Gas-Phase n-Butane Transfer Dehydrogenation via Silica-Supported Pincer-Iridium Complexes

Authors: Boris Sheludko, Cristina F. Castro, Chaitanya A. Khalap, Thomas J. Emge, Alan S. Goldman, and Fuat E. Celik

To be cited as: *ChemCatChem* 10.1002/cctc.202001399

Link to VoR: https://doi.org/10.1002/cctc.202001399

WILEY-VCH

FULL PAPER WILEY-VCH

Regioselective Gas-Phase *n*-Butane Transfer Dehydrogenation via Silica-Supported Pincer-Iridium Complexes

Boris Sheludko,[a],[b] Cristina F. Castro,[b] Chaitanya A. Khalap,[b] Thomas J. Emge,[a] Alan S. Goldman,*[a] Fuat. E. Celik*[b]

[a] Boris Sheludko, Dr. Thomas. J. Emge, Prof. Alan S. Goldman
Department of Chemistry and Chemical Biology
Rutgers, The State University of New Jersey
123 Bevier Road, Piscataway, NJ 08854
E-mail: alan.goldman@rutgers.edu

[b] Boris Sheludko, Cristina F. Castro, Chaitanya A. Khalap, Prof. Fuat E. Celik
Department of Chemical and Biochemical Engineering
Rutgers, The State University of New Jersey
98 Brett Road, Piscataway, NJ 08854
E-mail: fuat.celik@rutgers.edu

Abstract: The production of olefins via on-purpose dehydrogenation of alkanes allows for a more efficient, selective and lower cost alternative to processes such as steam cracking. Silica-supported pincer-iridium complexes of the form [(≡SiO-^{R4}POCOP)Ir(CO)] (^{R4}POCOP = κ^3-C_6H_3-2,6-$(OPR_2)_2$) are effective for acceptorless alkane dehydrogenation, and have been shown stable up to 300 °C. However, while solution-phase analogues of such species have demonstrated high regioselectivity for terminal olefin production under transfer dehydrogenation conditions at or below 240 °C, in open systems at 300 °C, regioselectivity under acceptorless dehydrogenation conditions is consistently low. In this work, complexes [(≡SiO-^{tBu4}POCOP)Ir(CO)] (**1**) and [(≡SiO-^{iPr4}PCP)Ir(CO)] (**2**) were synthesized via immobilization of molecular precursors. These complexes were used for gas-phase butane transfer dehydrogenation using increasingly sterically demanding olefins, resulting in observed selectivities of up to 77%. The results indicate that the active site is conserved upon immobilization.

Introduction

Olefins are versatile building blocks in the synthesis of various products spanning from fine chemicals to bulk polymers to fuels.[1] In contrast, alkanes are among the most inert organic species. Nevertheless, alkane activation is currently carried out on an industrial scale, typically at very high temperatures (600 – 1000 °C) that lead to reduced selectivity and formation of coke which, in between cycles, must be burned off prior to further reaction. Alkane dehydrogenation under milder conditions would be beneficial due to reduced energy demand and an opportunity to modulate the selectivity of the reaction.

Pincer-iridium complexes of the form [(^{R4}PCP)Ir] (^{R4}PCP = κ^3-C_6H_3-2,6-$(XPR_2)_2$; X = CH_2, O; R = ^{t}Bu, ^{i}Pr) have received great attention in the context of hydrocarbon functionalization and have found application in reactions such as alkane dehydrogenation and alkane metathesis among other C-H activation reactions,[2] dehydroaromatization,[3] and dehydrogenative C-C coupling.[4] Thermal (acceptorless) dehydrogenation can be performed using these species at rates of > 700 hr^{-1} at 200 °C.[2a-f, 2h-n] However, such processes are highly endothermic and thermodynamically unfavorable at lower temperatures. To counter this limitation, a sacrificial hydrogen acceptor may be added to the system to effect transfer dehydrogenation which is approximately thermoneutral.[2a-o]

We have previously shown that silica-supported pincer-iridium complexes are effective acceptorless dehydrogenation catalysts (Figure 1, top).[2i] The stability of such catalysts at elevated temperatures up to 300 °C arises from the concurrent generation of CO over these catalysts, which prevents thermal decomposition.[5] However, the selectivity of the system is unremarkable, resulting in an equilibrated mixture of product butenes (ca. 20% 1-butene) even at very low residence times, possibly due to rapid isomerization over the iridium species.[2i, 6] Previously, regioselectivity has been achieved using molecular pincer-iridium species in the heterogeneous (gas-solid) propene-butane transfer dehydrogenation of linear alkanes (e.g. up to ca. 65% 1-butene[2l]), even in gas-solid heterogeneous reactions, while also achieving turnovers up to 2000 hr^{-1} at early reaction times at 240 °C.[2l] However, at longer reaction times, the fraction of 1-alkene declines due to isomerization to generate internal butenes. To harness the intrinsic regioselectivity of such catalysts, one possible approach is to use a plug-flow reactor to shorten the residence time of the feed with the catalyst, thus limiting the amount of isomerization that takes place.

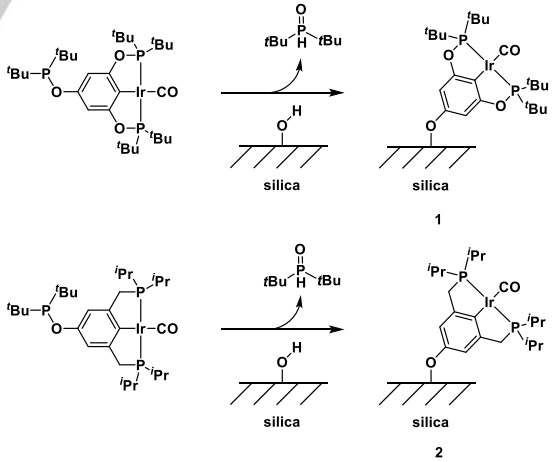

Figure 1. Silica-supported species **1** and **2** used in this work, prepared via immobilization of molecular precursors.

While previous work has made use of silica-tethered [(≡SiO-^{tBu4}POCOP)Ir(CO)] (**1**) in such continuous-flow systems, complexes based on the [(^{iPr4}PCP)Ir] framework are generally more active dehydrogenation catalysts presumably largely due to the less sterically hindered iridium environment. It has previously been shown that differences in the steric environment

of the iridium center significantly influence the activity of pincer-iridium species. For example, [(^{iPr4}PCP)Ir]-based catalysts typically show alkane dehydrogenation activities an order of magnitude or more greater than [(^{tBu4}PCP)Ir]-based catalysts.[7] In the model reaction of pentane-propene transfer dehydrogenation, the former complex achieved an initial rate of ca. 3800 TO hr^{-1} as compared with 120 TO hr^{-1} by the latter species.[2l] However, decreasing the size of the phosphinoalkyl substituents in complexes of type [(^{R4}PCP)Ir] (where R is smaller than *i*-Pr) can lead to formation of clusters in absence of a trapping ligand.[7a, 8] The site-isolation intrinsic to silica-supported pincer-iridium species appears to be a possible strategy that would allow easier access to such sterically unhindered iridium(I) species while mitigating intramolecular interactions leading to their dimerization or oligomerization. In pursuit of this, we chose to synthesize [(≡SiO-^{iPr4}PCP)Ir(CO)] (**2**) via tethering[9] of the molecular precursor [(*t*Bu$_2$PO-^{iPr4}PCP)Ir(CO)] and to explore the catalytic properties of the former in a model light-alkane dehydrogenation system at high temperatures (300 °C).

Results and Discussion

Synthesis of [(*t*Bu$_2$PO-^{iPr4}PCP)Ir(CO)]

Catalyst **2**, an analogue to [(^{iPr4}PCP)Ir] previously used in solution and gas/solid[2l] phase alkane dehydrogenation reactions, was synthesized in an attempt to obtain increased reactivity compared with **1**.[10]

The pre-catalyst [(HO-^{iPr4}PCP)IrHCl] was synthesized via metalation of the HO-^{iPr4}PCP ligand with [Ir(COD)Cl]$_2$. The ligand was synthesized via a protocol analogous to reported methods.[11] Recrystallization of the HCl complex from a solution in THF and hexanes at -30 °C led to formation of colorless X-ray quality crystals of THF-adduct [(HO-^{iPr4}PCP)IrHCl(THF)], which enabled verification of the proposed structure (See Supporting Information section S1[11] and figure 2). CCDC-2023539 contains the supplementary crystallographic data for this paper. These data can be obtained free of charge from The Cambridge Crystallographic Data Centre via www.ccdc.cam.ac.uk/data_request/cif.

The unit cell contains two conformational isomers. In both cases the THF and hydride ligands are mutually trans, consistent with their respective very weak and very strong trans influences.

The hydride and phosphorus atoms of [(HO-^{iPr4}PCP)IrHCl] afford signals at δ -37.13 and 58.08 ppm, in the ^{1}H and ^{31}P NMR spectra respectively, essentially equal to those previously reported for [(MeO-^{iPr4}PCP)IrHCl],[13] δ -37.06 and 58.68 ppm, and not very different from those for the unsubstituted analogue, [(^{iPr4}PCP)IrHCl],[2l] at δ -36.25 and 58.4 ppm. This suggests that the effect of varying the *para* substituent on the electronic environment of the iridium is likely to be relatively minor and the effect of varying the group bound to the O atom at the para position even more subtle. Thus replacing the hydroxyl group with either a phosphinite moiety or even a metal oxide surface such as silica is not expected to result in a significant change to the electronics of the metal center, in accord with previous observations.[14] The conclusion that the active site in the supported phase is essentially identical to that of solution-phase analogues is further supported with kinetic evidence below.

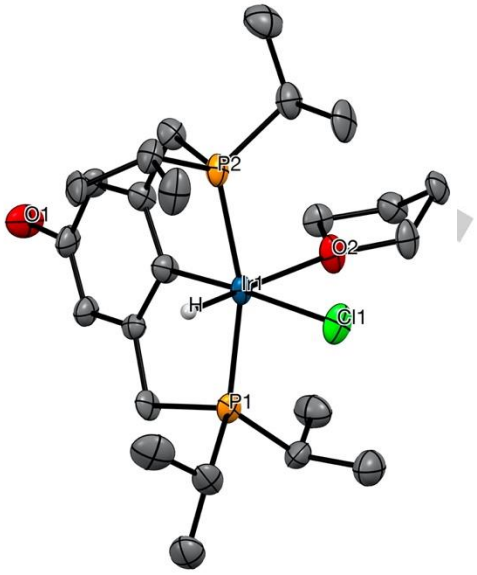

Figure 2. ORTEP diagram of novel pincer-iridium complex [(HO-^{iPr4}PCP)IrHCl(THF)] with thermal ellipsoids drawn at the 50% probability level. Only one molecule of the asymmetric unit cell is shown, and hydrogen atoms apart from ligand hydride are omitted for clarity. Selected bond lengths (Å) and bond angles (deg): Ir1-Cl1: 2.496(5), Ir1-P1: 2.284(4), Ir1-P2: 2,296(4), Ir1-C1: 2.03(2), Ir1-O2: 2.29(1), O1-C4: 1.41(2), C1-Ir1-Cl1: 175.8(5), P1-Ir1-P2: 162.7(2), C1-Ir1-O2: 90.6(6).

Alkane Transfer Dehydrogenation

Alkane dehydrogenation is a highly endergonic process and the occurrence of back reaction is a critical consideration in the experimental design. It is expected that a decreasing residence time would limit competition from the back reaction and, in the limit of *no* back reaction, the rate of the forward reaction may be measured accurately. Indeed, this ability to measure intrinsic reaction rates is one benefit of a plug-flow reactor setup.

Surprisingly, the product distribution arising from acceptorless butane dehydrogenation catalyzed by **1** at 340 °C was independent of the butane residence time over two orders of magnitude (τ = 0.0016 – 0.000064 mol$_{catalyst}$ min L^{-1}).[2i] Isomerization of 1-butene was studied over **1** and **2** in more detail, revealing rates of several thousand net forward turnovers per hour (Table S7).

In comparing the activity of **1** and **2** under transfer dehydrogenation conditions, the nature of the hydrogen acceptor and its partial pressure were varied. The three olefin hydrogen acceptors tested were ethylene, propene and 3,3-dimethyl-1-butene (*tert*-butylethylene, TBE). The carbonyl derivatives **1** and **2** were chosen since it was previously shown that the ethylene-bound analogues are converted to carbonyl-bound species under these reaction conditions and that the carbonyl species remains active for transfer dehydrogenation.[2i, 5] No leaching occurs under reaction conditions.[5] The summary of the kinetic results is presented in Table 1.

In all cases, the addition of a hydrogen acceptor depressed the activity in comparison to acceptorless dehydrogenation (Table 1, Figure 3). Given that olefin-bound complexes are not observed during reaction conditions at 300 °C,[5] this reduction in activity was likely a consequence of an increased CO concentration in the system, itself arising from the conversion of acceptor olefin used with trace water present.[2i] Although the rate of CO formation was too small to observe or measure, catalyst activity is has been demonstrated[5]to be very sensitive to CO pressure and, therefore, the rate may be expected to

decrease with increasing olefin content in the gas phase. When using TBE, the rate suppression was significantly more severe than with ethylene or propene. The mechanism of olefin hydration/decarbonylation to give CO is not fully understood but this may be attributable to more facile hydration of the intermediate branched olefin (e.g. the rate of isobutene hydration is ca. 100x faster than *n*-butene hydration at 115 °C[15]).

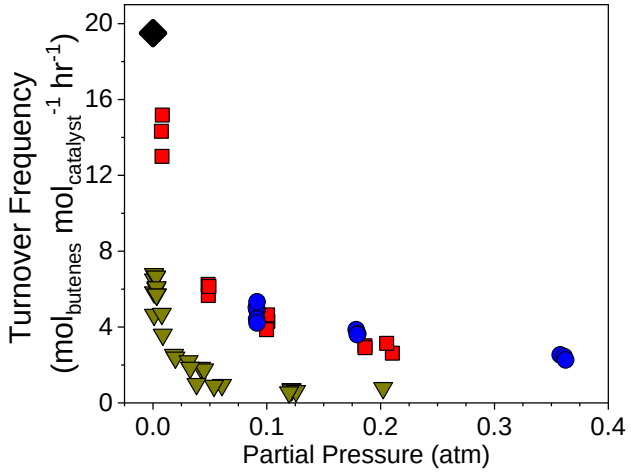

Figure 3. Transfer-dehydrogenation activity of catalyst **2** as a function of partial pressure of acceptor with various hydrogen acceptors: ethylene (●), propene (■) and TBE (▼).◆ represents the total turnover frequency for formation of butenes under acceptorless conditions. $\dot{V}_{total}$ = 80 mL min^{-1}, P_{butane} = 0.37 atm, $P_{acceptor}$ = 7.4 x 10^{-3} – 0.37 atm, P_{He} = 1.1 – 0.73 atm, P_{total} = 1.47 atm, T = 300 °C.

The results of transfer dehydrogenation of butane with propene as the hydrogen acceptor over catalysts **1** and **2** are shown in in Figure 4.

Catalyst **1** showed greater selectivity for 1-butene (~64-75%) production compared with acceptorless dehydrogenation at all tested pressures of propene. With **2**, the selectivity for 1-butene at low propene pressures was no different than under acceptorless conditions, but increased with propene pressure, reaching ~53% at 0.20 atm. Thus the presence of propene was found to substantially increase selectivity for 1-butene with both complexes by comparison to acceptorless dehydrogenation.

Steric crowding at the iridium center significantly impacts catalytic activity.[2l, 7a] *t*-Butyl substituted pincer ligands are far more crowded than the *i*-propyl analogues, and typically display much lower dehydrogenation rates.[2l, 7a] Accordingly, the measured activity of **1** was approximately an order of magnitude lower than that of **2** at propene pressures of 0.16 – 0.2 atm (0.15 vs 3 TO hr^{-1}) (Table 1).

The observed product distribution in alkane dehydrogenation by pincer-iridium is affected by two separate isomerization pathways (Figure 5).[2l] In the hydride isomerization pathway, 2,1-insertion of an α-olefin into an Ir-H bond of intermediate [(^{R4}PCP)IrH$_2$] leads to an isoalkyl species, which can reductively eliminate to yield internal olefin. In the allyl isomerization pathway, product α-olefin reacts directly with the 14e$^-$ [(^{R4}PCP)Ir] species to form an η^3-allyl complex, which can eliminate the internal olefin. The rates of both of these reactions can be compared to primary transfer dehydrogenation to explain the expected selectivity.[2l] Because both alkane addition and allyl formation result from reaction with [(^{R4}PCP)Ir], it is difficult to influence the rates of these two reactions independently. Increasing steric crowding at the reaction center impedes both reactions to a similar extent according to DFT calculations.[2l] The allyl pathway for isomerization therefore cannot be completely eliminated. The maximum achievable selectivity for a given catalyst therefore occurs in the absence of any contribution from the hydride isomerization pathway.

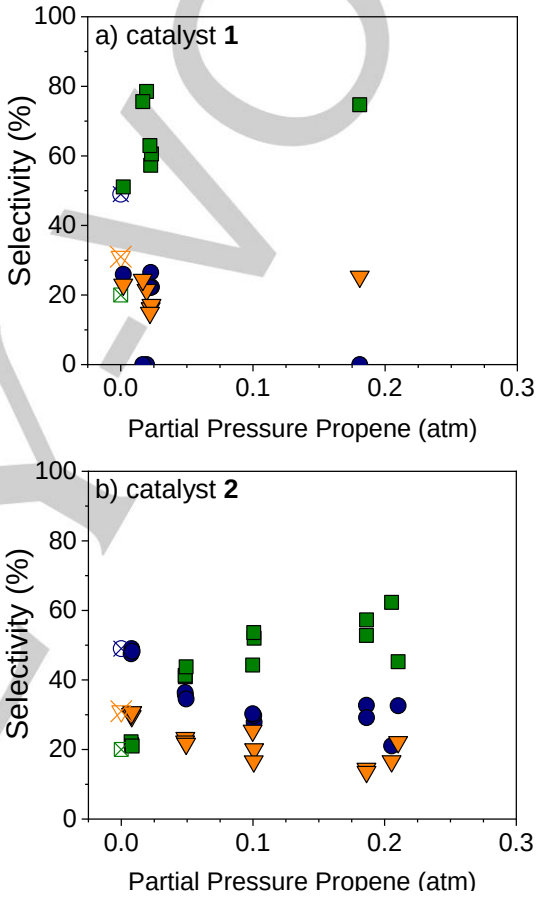

Figure 4. Product selectivities of 1-butene (■), *trans*-2-butene (●) and *cis*-2-butene (▼) from butane dehydrogenation as functions of propene partial pressure over (**a**) **1** and (**b**) **2**. Hollow shapes represent measured selectivities for 1-butene (⊠), *trans*-2-butene (⊗) and *cis*-2-butene (▽) under acceptorless dehydrogenation conditions. $\dot{V}_{total}$ = 80 mL min^{-1}, P_{butane} = 0.37 atm, P_{C3H6} = 7.4 x 10^{-3} – 0.22 atm, P_{He} = 1.1 – 0.88 atm, P_{total} = 1.47 atm, T = 300 °C.

Table 1. Summary of 1-butene selectivity and turnover frequency as a function of the catalyst used, the nature of the olefin acceptor and the partial pressure of the olefin.

Catalyst	Acceptor	Partial Pressure (atm)	1-butene Selectivity (%)	TOF ($mol_{butenes}^{-1}$ $mol_{catalyst}^{-1}$ hr^{-1})
1	N/A	N/A	20	8
2	N/A	N/A	20	19
2	Ethylene	0.08	48	5.3
2	Ethylene	0.31	52	2.6
2	Propene	0.007	22	14
2	Propene	0.20	53	3
1	Propene	0.007	64	0.54
1	Propene	0.16	75	0.15
2	TBE	0.001	21	6.51
2	TBE	0.23	18	1

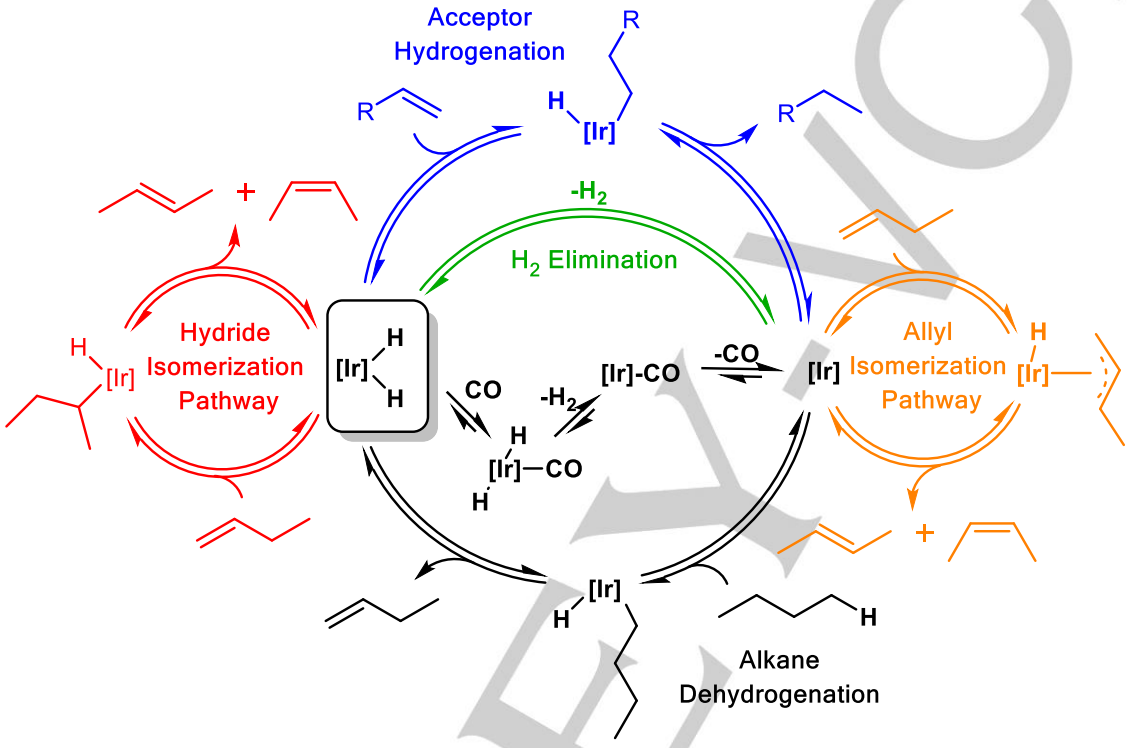

Figure 5. Proposed mechanistic pathways for observed product selectivities arising from butane dehydrogenation using supported pincer-iridium complexes.

Isomerization of 1-olefin by [(^{R4}PCP)IrH_2] competes with hydrogenation of olefin acceptor. It was previously reported that steric effects strongly impact the relative rates of these reactions. For example, in the case of [(^{tBu4}PCP)IrH_2] the barrier to isomerization of 1-hexene to 2-hexene was calculated to be 40.2 kJ/mol higher than that of propene hydrogenation. By contrast, for [(^{iPr4}PCP)IrH_2], the isomerization was calculated to have a barrier only 3.8 kJ/mol higher than propene isomerization. Thus higher partial pressures of propene inhibit the hydride isomerization pathway for [(^{iPr4}PCP)Ir], and likewise for its supported analogue **2**, resulting in increased yields of 1-butene (Figure 4b). For [(^{tBu4}PCP)IrH_2], the hydride pathway was calculated not to play a significant role in the isomerization; instead the allyl isomerization pathway predominated even at very low acceptor pressures. The relative rates of the isomerization pathway and dehydrogenation involve a competition for the 14e$^-$ pincer-Ir species (between alkane and 1-alkene product), which is unaffected by the concentration of propene. Likely for this reason, the percent yield of 1-butene is unaffected by the pressure of propene in the case of the bulky catalyst **1**. In other words, even at the lowest pressures of propene investigated, isomerization by the dihydride of **1** is almost completely eliminated, but the important allyl pathway is unaffected by propene at any partial pressure.

When using ethylene for transfer dehydrogenation of butane over **2**, the 1-butene selectivity was similarly found to increase by comparison to acceptorless dehydrogenation, but it did not appear to be a strong function of ethylene partial pressure (Figure 6). The selectivity (~52%) was approximately the same as at higher propene pressure in Figure 4b as both systems reached the same maximum. Closer investigation of the behavior at low partial pressures of ethylene was conducted in a separate experiment (Figure 7). Butane dehydrogenation over **2** was carried out with ethylene acceptor fed in very low concentrations. A cylinder containing a mixture of butane and ethylene was prepared, and this mixture was used as the gas feed. Due to the difference in vapor pressures, the ethylene was depleted over time, varying the partial pressure in the feed stream. This experiment showed that selectivity varied over a very small range, and by 7 × 10^{-5} atm has approximately

reached the maximum value. The near-independence of product distribution on ethylene pressure follows from the very facile hydrogenation of ethylene by [(^{iPr4}PCP)IrH$_2$], which was calculated to have a barrier 32.6 kJ/mol lower than that of 1-hexene isomerization by the same species.[2l] Thus at even very low pressures (ca. 7 × 10^{-5} atm or above) of ethylene, the butene product distribution is determined by a competition of butane dehydrogenation with isomerization by the allyl pathway, which is unaffected by acceptor.

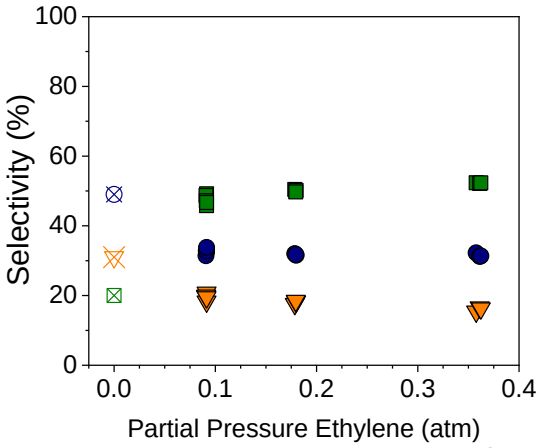

Figure 6. Product selectivities of 1-butene (■), *trans*-2-butene (●) and *cis*-2-butene (▼) from butane dehydrogenation over **2** as functions of ethylene partial pressure. Hollow shapes represent measured selectivities for 1-butene (☒), *trans*-2-butene (⊗) and *cis*-2-butene (⋈) under acceptorless dehydrogenation conditions. $\dot{V}_{total}$ = 80 mL min^{-1}, P_{butane} = 0.37 atm, P_{C2H4} = 0.09 – 0.37 atm, P_{He} = 1.01 – 0.73 atm, P_{total} = 1.47 atm, T = 300 °C.

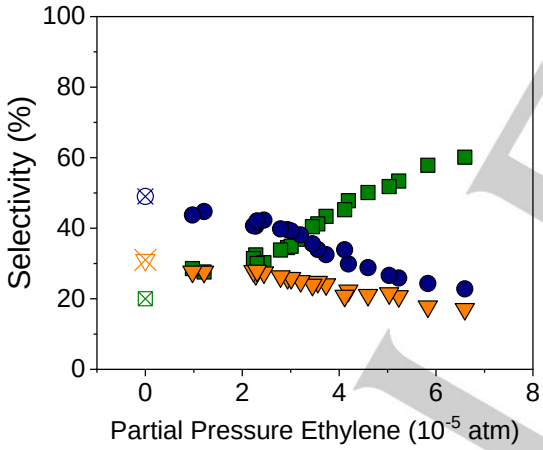

Figure 7. Product selectivities of 1-butene ( ), *trans*-2-butene ( ) and *cis*-2-butene (▼) from butane dehydrogenation over **2** as functions of ethylene partial pressure. Hollow shapes represent measured selectivities for 1-butene (☒), *trans*-2-butene (⊗) and *cis*-2-butene (⋈) under acceptorless dehydrogenation conditions. $\dot{V}_{total}$ = 80 mL min^{-1}, P_{butane} ≈ 0.37 atm, P_{C2H4} = 6.5 x 10^{-5} – 9.7 x 10^{-6} atm, P_{He} ≈ 1.1 atm, P_{total} = 1.47 atm, T = 300 °C.

In contrast with ethylene and propene, TBE showed no effect on product selectivity over **2** as a function of partial pressure (Figure 8). Again, this is well rationalized by prior DFT calculations on the unsupported species. TBE hydrogenation was calculated to have a barrier 15.9 kJ/mol higher than 1-hexene isomerization by [(^{iPr4}PCP)IrH$_2$].[2l] Thus extensive isomerization by the supported analogue of this species (in addition to isomerization by the supported analogue of [(^{iPr4}PCP)Ir]) via the allyl pathway) results in a thermodynamic distribution of butene isomers as is observed in the absence of acceptor.

To determine whether acceptorless dehydrogenation contributes to the activity observed in the previous experiments, a ratio β was devised to compare the rates of butene formation and acceptor hydrogenation. If the reaction proceeds solely by transfer dehydrogenation, these amounts are equal and β is equal to one. A value less than one indicates that consumption of the acceptor is outpaced by dehydrogenation, so acceptorless dehydrogenation must also be taking place in the system. The results are plotted in Figure 9.

In the case of ethylene as acceptor, β was approximately one at 0.1 atm of ethylene and above, indicating a strong preference for the reaction to proceed solely via transfer dehydrogenation. At very low ethylene partial pressures (Figure S4) both β and 1-butene selectivity were significantly lower. Propene showed similar behavior. At higher partial pressure, in the same range where selectivity was maximized, β was approximately one. Below 0.1 atm propene, β was less than one, coinciding with lower yields of 1-butene due to isomerization by dihydride. In the case of TBE as hydrogen acceptor, the acceptor hydrogenation was never competitive with hydride isomerization, and acceptorless dehydrogenation dominated the activity as well, with β < 0.5 at all partial pressures.

Thus a low rate of acceptor hydrogenation results in a low value for β and a low observed selectivity for 1-butene production due to an increased contribution to olefin isomerization by the iridium dihydride. By extension, it is then expected that acceptorless dehydrogenation conditions (β = 0), would show low selectivity for 1-butene production as well, consistent with our previously reported results with supported pincer-iridium complexes.[2i, 5]

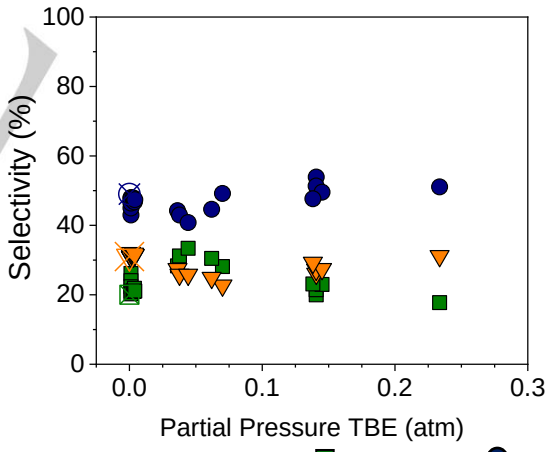

Figure 8. Product selectivities of 1-butene (■), *trans*-2-butene (●) and *cis*-2-butene (▼) from butane dehydrogenation over **2** as functions of TBE partial pressure from 0.08 – 16 mol%. Hollow shapes represent measured selectivities for 1-butene (☒), trans-2-butene (⊗) and cis-2-butene (⋈) under acceptorless dehydrogenation conditions. $\dot{V}_{total}$ = 80 mL min^{-1}, P_{butane} = 0.37 atm, P_{TBE} = 1.0 x 10^{-3} – 0.23 atm, P_{He} = 1.1 – 0.87 atm, P_{total} = 1.47 atm, T = 300 °C.

In the analysis above, we relied on mechanistic studies[2l] of solution-phase dehydrogenation systems with a number of key differences from those in the present study. In this work, the pincer-iridium complexes were CO-ligated and covalently anchored to a silica surface. Nevertheless, the results were completely consistent with those calculated by DFT for alkane dehydrogenation by unsubstituted pincer-iridium complexes,

unbound to any support and not bound to CO, in vacuo at lower temperature. This highlights the chemical equivalence of the present system to more familiar unsupported systems containing the same active site.

Further, these results show that the immobilization procedure previously used for bulkier pincer-iridium complexes may be extended to those species containing less crowded active sites, informing future catalyst design and allowing for the study of more active such analogues.

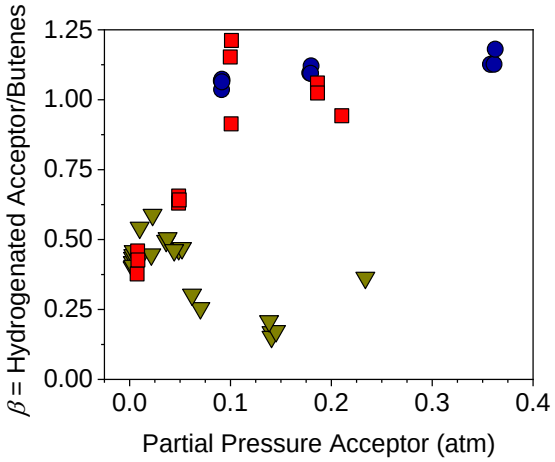

Figure 9. Ratio of hydrogenated acceptor to total butenes formed over **2** using ethylene (●), propene (■) and TBE (▼). $\dot{V}_{total}$ = 80 mL min^{-1}, P_{butane} = 0.37 atm, $P_{acceptor}$ = 0 – 0.37 atm, P_{He} = 1.1 – 0.73 atm, P_{total} = 1.47 atm, T = 300 °C.

Conclusion

In summary, we present here the first report of transfer dehydrogenation effected by a silica-tethered pincer-iridium system based on the [(^{iPr4}PCP)Ir] framework.[10] As previously reported for unsupported complexes, the use of a rapidly hydrogenated acceptor results in higher selectivity for 1-alkene formation by preventing olefin isomerization via the pincer-iridium dihydride intermediate. Dehydrogenation rates were lower at higher partial pressures of olefinic hydrogen acceptor, likely caused by an increase in CO production. Terminal olefin selectivity up to 75% was observed with a (^{tBu4}POCOP) derivative, and ca. 53% was observed with an (^{iPr4}PCP) derivative. The experimental results with supported species are consistent with a mechanistic model previously developed for solution-phase analogues and provide evidence for equivalence of the shared active site.

Experimental Section

Catalyst Preparation

All chemical syntheses and material preparations were performed under an air-free argon atmosphere unless otherwise noted. Complex [(tBu$_2$PO-^{tBu4}POCOP)Ir(CO)] was synthesized, and supported **1** was prepared, according to previously established procedures.[2i]

Calcination of support materials was carried out under dry air in a 6.4 mm outer diameter (OD) quartz tube reactor with an expanded section of 12.5 mm OD packed with quartz wool to hold the catalyst powder in place. After calcination, the powder was flushed of air prior to being brought into an argon glovebox for further use. Supports were calcined to 550 °C with a ramp rate of 2 °C/min and a hold of five hours at temperature.

Synthesis of [(tBu$_2$PO-^{iPr4}PCP)Ir(CO)]

Synthesis of the precursor ligand HO-^{iPr4}PCP was carried out by analogy to literature methods.[11] Tetrahydrofuran (THF) and methanol were distilled over Na/K alloy. All other solvents were purchased anhydrous and used as received. Cyclooctadiene was purified by distillation under argon to remove heavy impurities. Anhydrous triethylamine, di-*iso*-propylphosphine and chloro-di-*tert*-butylphosphine were used as received. Solution-phase ^{1}H and ^{31}P NMR spectra were collected using either a Bruker Avance III operating at 400 MHz for ^{1}H NMR or 162 MHz for ^{31}P{^{1}H} NMR or a Varian VNMRS operating at 500 MHz for ^{1}H NMR or 202 MHz for ^{31}P(^{1}H) NMR.

Synthesis of 3,5-dihydroxymethylphenol[11]

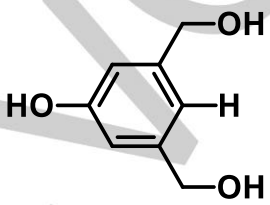

To a round-bottom flask on ice containing a slurry of 2.71 g (7.14 x 10^{-2} mol) lithium aluminum hydride in 40 mL tetrahydrofuran was slowly added 5.00 g (2.38 x 10^{-2} mol) of dimethyl 5-hydroxyisophthalate as a solution in 80 mL tetrahydrofuran via cannula needle. The slurry became a yellow-green color which was then refluxed 16 hours in an oil bath at 90 °C. At the end of this time, the reaction was allowed to cool to room temperature and then put on ice, at which point it was quenched with 1M hydrochloric acid to a pH = 3. The reaction mixture was then filtered of solids and extracted 4 x 50 mL with ethyl acetate. These fractions were then combined and dried over sodium sulfate, filtered again and the solvent was removed in vacuo to yield a viscous yellow oil (1.72 g, 1.11 x 10^{-2} mol, 46.6 % yield). Identity of the product was confirmed by comparison to reported NMR spectra.[11b]

Synthesis of 3,5-dibromomethylphenol[11]

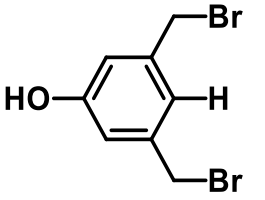

To a Schlenk flask equipped with a stir bar was added 10 mL sulfolane and 2.2 mL (6.27 g, 2.32 x 10^{-2} mol) phosphorus tribromide and cooled in an ice bath after addition. To a second Schlenk flask was added 10 mL sulfolane and 1.717 g (1.11 x 10^{-2} mol) 3,5-dihydroxymethylphenol. The contents of this flask were cannula-transferred into the first flask and sealed under argon for three days. At the end of this time, the reaction mixture was unsealed and poured into 100 mL of ice water. It was then saturated with sodium chloride and extracted 3 x 50 mL with diethyl ether. The organic fractions were combined and washed 2 x 50 mL with brine before being dried over sodium sulfate and filtered. Finally, the diethyl ether was removed in vacuo to yield a crude yellow oil. The final product (1.82 g, 46 %) was isolated

via column chromatography using a 3:1 hexanes:diethyl ether solvent. Identity of the product was confirmed by comparison to reported NMR spectra.[11b]

Synthesis of 3,5-di-*iso*-propylphosphinomethylphenol (HO-^{iPr4}PCP-H)[11]

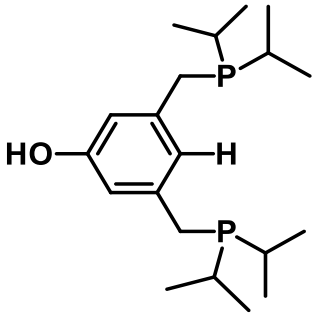

In a Schlenk flask equipped with a stir bar was dissolved 1.0 g (3.57 mmol) 3,5-dibromomethylphenol in 40 mL of freshly dried, degassed methanol. To this solution was added 0.8685 g di-*iso*-propylphosphine (7.32 mmol, ca. 1.3 mL) and the reaction mixture was refluxed for three days, at the end of which the solution was a clear, amber color. The reaction was cooled to room temperature and 3 mL triethylamine was added and allowed to stir for ca. 1 hour, after which the solvent was removed under vacuum to yield an off-yellow solid. The residue was washed 1 x 10 mL acetone and then extracted 3 x 10 mL pentane, with the organic fractions being combined and the solvent removed to yield crude product. This was then recrystallized from a highly concentrated diethylether solution layered with pentane to yield the final product as white crystals (1.02 g, 3.38 mmol, 94 %). Identity of the product was confirmed by comparison to reported NMR spectra.[11b]

Synthesis of [(HO-^{iPr4}PCP)IrHCl]

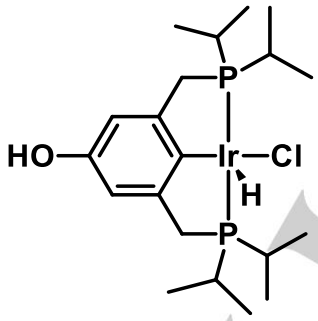

In a Schlenk flask charged with a stir bar was dissolved 0.414 g (1.17 mmol) 3,5-di-*iso*-propylphosphinomethylphenol and 0.393 g (0.585 mmol) $[Ir(COD)Cl]_2$ in benzene. The flask was put under a flow of hydrogen and then heated to reflux temperature, during which the mixture became orange with some white precipitate. Refluxing for 16 hours resulted in a deep red solution with some black precipitate present on the flask walls. The solution was cooled to room temperature and solvent was removed in vacuo to yield a dark red solid. The residual solid was washed with toluene and the supernatant was filtered through a 0.2 μm syringe filter. The material was recrystallized from a concentrated solution of THF layered with pentane at -30 °C to yield white crystals which were determined to be the six-coordinate adduct [(HO-^{iPr4}PCP)IrHCl(THF)] via X-ray diffraction. Upon dissolution in toluene, the THF rapidly dissociated to regenerate a solution of 1:1 THF:[(HO-^{iPr4}PCP)IrHCl] as determined by ^{1}H NMR. Removal of solvent at this point allowed for isolation of pure final product.

^{1}H NMR (400 MHz, C_6D_6) δ 6.50 (s, 2H, Ar-**H**), 4.42 (bs, 1H, O-**H**), 2.778 (d of vt, J_{PH} = 4 Hz, J_{HH} = 18.4 Hz, 2H, Ar-C**H**$_2$P), 2.689 (d of vt, J_{PH} = 4 Hz, J_{HH} = 16.8 Hz, 2H, Ar-C**H**$_2$P), 2.676 (m, 2H, PC**H**$(CH_3)_2$), 1.98 (m, 2H, PC**H**$(CH_3)_2$), 1.22 (m, 12H, PCH$(C\mathbf{H}_3)_2$), 0.92 (app. sext, 7.6 Hz, 12H, PCH$(C\mathbf{H}_3)_2$), -37.13 (s, 1H, Ir-**H**). ^{31}P NMR (162 MHz, C_6D_6) δ 58.08.

Synthesis of [(*t*Bu$_2$PO-^{iPr4}PCP)Ir(C_2H_4)]

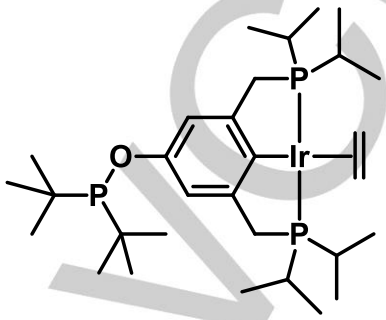

To a Schlenk flask equipped with a reflux condenser and a stir bar was added 150.8 mg (0.259 mmol) [(HO-^{iPr4}PCP)IrHCl] and 58.8 mg (0.524 mol) potassium *tert*-butoxide. The flask was put under ethylene flow and, after 5 minutes, 10 mL toluene was added down the condenser. The solution immediately turned colorless and then reddish-brown. The solution was allowed to stir at 30 °C for 30 minutes. At this point, 1 mL (0.79 g, 0.544 mmol) chloro-di-*tert*-butylphosphine was added followed by ca. 2 mL of toluene and the reaction was allowed to reflux for 16 hours to yield a reddish-green solution. The solvent was then removed and the residue was extracted with 3 x 5 mL toluene and filtered through a 0.2 um syringe filter. The organics were combined and dried in vacuo to yield the pure final product as a very dark reddish brown powder in quantitative yield.

^{1}H NMR (400 MHz, C_6D_6) δ 7.39 (s, 2H, Ar-**H**), 3.04 (app. t, 4 Hz, 4H, $C_2\mathbf{H}_4$), 3.00 (t, 3.2 Hz, 4H, Ar-C**H**$_2$P), 2.00 (app. tp, 2.4 Hz, 7.2 Hz, 4H, PC**H**$(CH_3)_2$), 1.26 (d, 11.5 Hz, 18H, PC$(C\mathbf{H}_3)_3$), 1.051 (app. q (dd), 3.6 Hz, 12H, PH$(C\mathbf{H}_3)_2$), 0.894 (app. q (dd), 6.4 Hz, 12H, PH$(C\mathbf{H}_3)_2$). ^{31}P NMR (162 MHz, C_6D_6) δ 148.92, 49.26.

Synthesis of [(*t*Bu$_2$PO-^{iPr4}PCP)Ir(CO)]

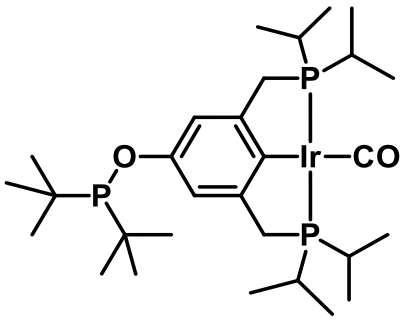

[(*t*Bu$_2$PO-^{iPr4}PCP)Ir(C_2H_4)] was synthesized as above, after which the crude product from reaction was transferred to a Kontes flask, which was then evacuated and charged with carbon monoxide. The solution was allowed to stir for 10 minutes, during which it turned yellow-brown. All gas was removed via one freeze-pump-thaw cycle and the flask was

again charged with carbon monoxide and allowed to stir a further 30 minutes. The solution was then dried in vacuo to yield a yellow-brown powder that was determined to be 70% pure by ^{31}P NMR and used without further purification. The major impurity present was found to be di-*tert*-butylphosphine oxide.

^{1}H NMR (500 MHz, C_6D_6) δ 7.33 (s, 2H, Ar-**H**), 3.16 (s, 4H, Ar-C**H**$_2$P), 1.98 (bs, 4H, PC**H**$(CH_3)_2$), 1.243 (d, 11.5 Hz, 18H, PC(C**H**$_3)_3$), 1.168 (q, 8 Hz, 12H, PH(C**H**$_3)_2$), 0.918 (q, 7 Hz, 12H, PH(C**H**$_3)_2$). ^{31}P NMR (202 MHz, C_6D_6) δ 149.51, 67.39.

Gas-phase Continuous-flow Catalytic Data

Reactions were carried out in a 6.4 mm outer diameter (OD) quartz tube reactor with an expanded section of 12.5 mm OD packed with quartz wool to hold the catalyst powder in place. The reactor was packed with supported catalyst under argon atmosphere and sealed with valves prior to connection to the gas-flow manifold. The reactor was placed inside a resistively heated ceramic furnace with external temperature control, and the catalyst bed temperature was measured with a K-type thermocouple placed in direct contact with the catalyst powder. The tubing upstream of the reactor was purged with helium gas prior to opening the reactor to the manifold.

Butane (Airgas, 99.99%) was used as received. Helium (Praxair, 99.999%) was passed through an on-stream oxygen and moisture trap. Helium was bubbled through a stainless-steel saturator filled with 3,3-dimethyl-1-butene (*tert*-butylethylene, TBE) to provide the desired vapor pressure. Reaction products were analyzed using an Agilent 7890B GC equipped with a GS-GASPRO capillary column (0.32 mm x 60 m) fitted with a flame ionization detector.

In a typical experiment, 2 mg of molecular pincer-iridium complex [(*t*Bu$_2$PO-^{tBu4}POCOP)Ir(CO)] or [(*t*Bu$_2$PO-^{iPr4}PCP)Ir(CO)] was supported on 60 mg of silica support via incipient wetness impregnation and the resulting material was used without further treatment. Unless stated otherwise, all experiments were carried out at 1.47 atm total pressure due to pressure drop through the catalyst bed. Gas flow rates reported were measured at room temperature and pressure.

Selectivity was calculated via:

$$S_i = x_i / \Sigma x_i \cdot 100\%$$

(x_i = mol fraction of product)

Acknowledgements

This work was supported by the National Science Foundation (CBET-1705746) and the Department of Energy Office of Science (DE-SC0020139). The authors would like to thank Prof. Akshai Kumar for valuable discussions, and Chenxu Liu and Cesar A. Rubio for their help in data processing.

Keywords: iridium • dehydrogenation • hydrogen transfer • heterogeneous catalysis • supported catalysts

[1] J. Sattler, J. Ruiz-Martinez, E. Santillan-Jimenez, B. M. Weckhuysen, *Chem. Rev.* **2014**, *114*, 10613-10653.

[2] a) A. Kumar, T. M. Bhatti, A. S. Goldman, *Chem. Rev.* **2017**, *117*, 12357-12384; b) J. Choi, A. S. Goldman, in *Iridium Catalysis* (Ed.: P. G. Andersson), Springer Berlin Heidelberg, Berlin, Heidelberg, **2011**, pp. 139-167; c) D. Morales-Morales, *Pincer Compounds, Chemistry and Applications*, 1st ed., Elsevier, **2018**; d) C. M. Jensen, *Chem. Comm.* **1999**, 2443-2449; e) I. Göttker-Schnetmann, P. White, M. Brookhart, *J. Am. Chem. Soc.* **2004**, *126*, 1804-1811; f) I. Göttker-Schnetmann, P. S. White, M. Brookhart, *Organometallics* **2004**, *23*, 1766-1776; g) W. Yao, Y. Zhang, X. Jia, Z. Huang, *Angew. Chem. Int. Ed.* **2014,** *53*, 1390-1394**;** h) K. E. Allen, D. M. Heinekey, A. S. Goldman, K. I. Goldberg, *Organometallics* **2013**, *32*, 1579-1582; i) B. Sheludko, M. T. Cunningham, A. S. Goldman, F. E. Celik, *ACS Catal.* **2018**, *8*, 7828-7841; j) A. R. Chianese, M. J. Drance, K. H. Jensen, S. P. McCollom, N. Yusufova, S. E. Shaner, D. Y. Shopov, J. A. Tendler, *Organometallics* **2014**, *33*, 457-464; k) A. R. Chianese, A. Mo, N. L. Lampland, R. L. Swartz, P. T. Bremer, *Organometallics* **2010**, *29*, 3019-3026; l) A. Kumar, T. Zhou, T. J. Emge, O. Mironov, R. J. Saxton, K. Krogh-Jespersen, A. S. Goldman, *J. Am. Chem. Soc.* **2015**, *137*, 9894-9911; m) A. Kumar, J. D. Hackenberg, G. Zhuo, A. M. Steffens, O. Mironov, R. J. Saxton, A. S. Goldman, *J. Mol. Catal. A. Chem.* **2016**; n) Z. Huang, E. Rolfe, E. C. Carson, M. Brookhart, A. S. Goldman, S. H. El-Khalafy, A. H. R. MacArthur, *Adv. Synth. Catal.* **2010**, *352*, 125-135; o) J. Choi, A. H. MacArthur, M. Brookhart, A. S. Goldman, *Chem. Rev.* **2011**, *111*, 1761-1779; p) D. Hermann, M. Gandelman, H. Rozenberg, L. J. W. Shimon, D. Milstein, *Organometallics* **2002**, *21*, 812-818; q) E. Ben-Ari, M. Gandelman, H. Rozenberg, L. J. W. Shimon, D. Milstein, *J. Am. Chem. Soc.* **2003**, *125*, 4714-4715; r) E. Ben-Ari, G. Leitus, L. J. W. Shimon, D. Milstein, *J. Am. Chem. Soc.* **2006**, *128*, 15390-15391; s) Y. Wang, L. Qian, Z. Huang, G. Liu, Z. Huang, *Chin. J. Chem.* **2020**, *38*, 837-841; t) X. Zhang, S.-B. Wu, X. Leng, L. W. Chung, G. Liu, Z. Huang, *ACS Catal.* **2020**, *10*, 6475-6487; u) X. Jia, L. Zhang, C. Qin, X. Leng, Z. Huang, *Chem. Comm.* **2014**, *50*, 11056-11059. v) H. Valdés, E. Rufino-Felipe, D. Morales-Morales, *J. Organomet. Chem* **2019**, *15*, 120864. w) H. Valdés, M. A. García-Eleno, D. Canseco-Gonzalez, D. Morales-Morales, *ChemCatChem* **2018**, *10*, 3136-3172.

[3] R. Ahuja, B. Punji, M. Findlater, C. Supplee, W. Schinski, M. Brookhart, A. S. Goldman, *Nat. Chem.* **2010**, *3*, 167.

[4] M. Wilklow-Marnell, B. Li, T. Zhou, K. Krogh-Jespersen, W. W. Brennessel, T. J. Emge, A. S. Goldman, W. D. Jones, *J. Am. Chem. Soc.* **2017**, *139*, 8977-8989.

[5] B. Sheludko, C. F. Castro, A. S. Goldman, F. E. Celik, *ACS Catal.* **2020**, DOI: 10.1021/acscatal.0c02406.

[6] Y. Wang, C. Qin, X. Jia, X. Leng, Z. Huang, *Angew. Chem. Int. Ed.* **2017**, *56*, 1614-1618.

[7] a) S. Kundu, Y. Choliy, G. Zhuo, R. Ahuja, T. J. Emge, R. Warmuth, M. Brookhart, K. Krogh-Jespersen, A. S. Goldman, *Organometallics* **2009**, *28*, 5432-5444; b) F. C. Liu, A. S. Goldman, *Chem. Comm.* **1999**, 655-656.

[8] J. M. Goldberg, G. W. Wong, K. E. Brastow, W. Kaminsky, K. I. Goldberg, D. M. Heinekey, *Organometallics* **2015**, *34*, 753-762.

[9] B. C. Vicente, Z. Huang, M. Brookhart, A. S. Goldman, S. L. Scott, *Dalton Trans.* **2011**, *40*, 4268-4274.

[10] O. S. Mironov, R. J. Saxton, A. S. Goldman, A. Kumar, US10017430B2, February 15, 2018.

[11] a) N. Ashkenazi, A. Vigalok, S. Parthiban, Y. Ben-David, L. J. W. Shimon, J. M. L. Martin, D. Milstein, *J. Am. Chem. Soc.* **2000**, *122*, 8797-8798; b) A. Dauth, U. Gellrich, Y. Diskin-Posner, Y. Ben-David, D. Milstein, *J. Am. Chem. Soc.* **2017**, *139*, 2799-2807.

[12] a) APEX2, SAINT and SADABS. Bruker AXS Inc. Madison, WI, USA. **2013**. b) G. M. Sheldrick, *Acta Cryst.* **2008**, A64, 112-122. c) A. Bondi, *Journal of Physical Chemistry C* **1964**, *68(3)*, 441-451.

[13] K. Zhu, P. D. Achord, X. Zhang, K. Krogh-Jespersen, A. S. Goldman, *J. Am. Chem. Soc.* **2004**, *126*, 13044-13053.

[14] Z. Huang, M. Brookhart, A. S. Goldman, S. Kundu, A. Ray, S. L. Scott, B. C. Vicente, *Adv. Synth. Catal.* **2009**, *351*, 188-206.

[15] K. Deguchi, I. Yuhara, S. Ogasawara, *Nippon Kagaku Kaishi* **1974**, *1974*, 319-324.

Entry for the Table of Contents

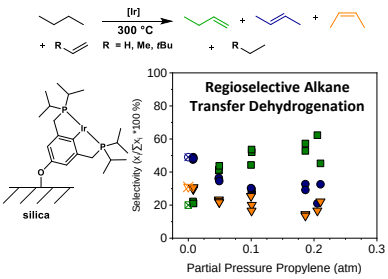

Silica-immobilized pincer-iridium complexes may be used for alkane-olefin transfer dehydrogenation, reaching terminal olefin selectivities of 70 % with a sufficiently unhindered hydrogen acceptor. The increased regioselectivity results from inhibition of the hydride isomerization pathway, previously implicated for analogous, molecular solution-phase species. This result is consistent with preservation of the iridium active site upon tethering.